Journal of Non-Crystalline Solids 357 (2011) 3726–3733

Contents lists available at ScienceDirect

Journal of Non-Crystalline Solids

journal homepage: www.elsevier.com/ locate/ jnoncrysol

Crystallisation kinetics, glass forming ability and thermal stability in glassy $Se_{100-x}In_x$ chalcogenide alloys

Cosmas M. Muiva [a,c,*], Stephen T. Sathiaraj [a,c], Julius M. Mwabora [b,c]

[a] Department of Physics, University of Botswana, P/Bag UB-0022, Gaborone, Botswana
[b] Department of Physics, University of Nairobi, P.O. Box 30197, GPO-00100 Nairobi, Kenya
[c] African Materials Science and Engineering Network (AMSEN), University of Botswana Node, P/Bag UB-0022, Gaborone, Botswana

ARTICLE INFO

Article history:
Received 19 March 2011
Received in revised form 23 July 2011
Available online 20 August 2011

Keywords:
Se–In;
DSC;
Chalcogenides;
Crystallisation kinetics;
Thermal stability

ABSTRACT

Differential scanning calorimetry (DSC) studies have been done under non-isothermal conditions at different heating rates for glassy $Se_{100-x}In_x$ ($5 \le x \le 20$) alloys. DSC traces with well-defined endothermic and exothermic troughs and peaks at glass transition (T_g), crystallisation (T_c) and melting (T_m) temperatures were observed. The crystallisation kinetics parameters, Avrami index (n), activation energy for crystallisation (E_c) and frequency factor (K_o), have been calculated on the basis of the classical Johnson–Mehl–Avrami (JMA) model and related methods derived by Kissinger, Augis–Bennett and Mahedevan. Activation energy for glass transformation (E_t) has been evaluated on the usual two different non-isothermal methods developed by Moynihan and Kissinger. An extension of the Augis–Bennett method well known for evaluating E_c to calculate E_t has been explored with satisfactory results. Results obtained from these methods are in close agreement with each other. Close correlation between E_t, E_c and heating rate (β) was observed. The glass forming ability (GFA) and thermal stability parameters have been calculated for each glass system. It was found that the proportion of indium additive changed significantly the values of glass/crystal transformation, GFA and thermal stability of the studied system.

1. Introduction

Semiconducting chalcogenide glasses are interesting materials belonging to the inorganic disordered solids. These glasses have recently been the subject of intense research both for basic physics understanding as well as targets for device fabrication owing to their easily modifiable electrical, optical and thermal properties. Alloying of more electropositive elements (In, Bi, Cd, Pb, Sb, Ge, Ag, Sn and As) with chalcogenide elements (S, Se and Te) has been reported in literature [1,2]. Of these Se based chalcogenide alloys are the most versatile materials in terms of composition and preparative conditions and have wide potential for technological applications in solid state devices. Applications include xerography, vidicon pick up tubes, reversible optical recording and electrical threshold switching [3–5]. Amorphous selenium is assumed to consist of two structural arrangements, long chains and Se_8 rings in a mixture held by presumably weak Van der Waal's forces with strong covalent bonding between the atoms in the chains or rings [6]. These molecular bonds imply that these glasses are less robust and mechanically weaker than oxide glasses. Moreover, the amorphous phase of Se is associated with a short lifetime, low sensitivity (nucleation and crystallisation rates) and low thermal stability and thus poses limited applications. Additives are significant in increasing thermal stability, sensitivity, thermal and electrical conductivity, lifetime and glass transition temperature. The crystallisation kinetics in binary Se based glasses have been investigated by various workers using the non-isothermal differential scanning calorimetry (DSC) technique, (Se–Sb) [2], (Se–Bi) [7], (Se–S) [8], (Se–Ge) [9], (Ga–Se) [10], (Se–As) [11] and (Se–In, Se–Te) [12], which allows measurement of heat flow to a sample laded pan against an empty reference pan in a cycle where the two are heated at a constant rate. The glass transition and crystallisation arise from molecular relaxations and structural rearrangements from one state of stability, usually metastable, to a more stable configuration in which enthalpy and specific heat capacity are altered. These changes appear in a DSC trace as endothermic or exothermic troughs and peaks respectively. Crystallisation kinetics studies give insight into transport mechanism, glass forming ability (GFA), thermal stability and range of temperature for transformation from amorphous to crystalline which is an important knowledge in technological applications based on glassy, crystalline states or reversible transformations. Little has been found in literature on the crystallisation kinetics in Se–In despite this material being a platform for a wide range of technological applications [13,14]. In this study, diverse quantitative methods have been applied to study glass transition/crystallisation kinetics, glass forming ability as well as thermal stability of $Se_{100-x}In_x$ ($x = 5, 10, 15, 20$) alloys under non-isothermal conditions.

* Corresponding author at: Department of Physics, University of Botswana, P/Bag UB-0022, Gaborone, Botswana. Tel.: +267 355 2618; fax: +267 318 5097.
E-mail address: cmuiva@yahoo.co.uk (C.M. Muiva).

0022-3093/$ – see front matter © 2011 Elsevier B.V. All rights reserved.
doi:10.1016/j.jnoncrysol.2011.07.033

2. Experimental details

The bulky samples of $Se_{100-x}In_x$ ($x=5, 10, 15, 20$) were prepared by the well-known melt quenching technique. 99.999% pure In and Se were weighed into precleaned silica ampoules of internal diameter 20 mm and length 80 mm to make a total batch of 4 g. The ampoules, initially evacuated to 10^{-5} mbar, were sealed in Argon ambient at a pressure of 10^{-2} mbar. The samples were then transferred to a furnace where the temperature was raised in steps of 10 K/min to 950 K which is way above the melting points of In and Se and held at this temperature for 12 hours with periodic vigorous agitation to ensure complete fusing and homogeneity of the alloys. The hot ampoules were then removed and rapidly transferred to ice cold water for quenching. To ensure uniform cooling of the batch, all the ampoules were arranged linearly at equidistant separation in a rectangular copper net. The hot ampoule containing basket was rapidly transferred to a large ice cold water bath. The bulk samples were then ground to a fine powder for further analysis.

The glassy nature was confirmed by using powder X-ray diffraction (PXRD) data obtained from a Philips PW 3710 XRD system fitted with a copper anode ($\lambda=1.54$ Å) and scanned in the range of 2θ values from 5 to 90°. Glass crystallisation kinetics were studied from data obtained from a Rigaku Model 8230 differential scanning calorimeter in the heating rates 5, 10, 15, and 20 K/min. The temperature accuracy of the instrument was ± 0.1 K with heat flow accuracy of ± 0.01 mW. The instrument was calibrated using In, Sn and Pb standards of known heat capacity and melting points. Glass transition temperature (T_g), onset of crystallisation (T_o), peak crystallisation (T_c) and peak melting temperatures (T_m) were determined from the microprocessor of the thermal scanner.

3. Theoretical basis

Crystallisation kinetics in amorphous materials has been studied using the classical Johnson–Mehl–Avrami (JMA) model [15–17]. According to this model, the crystallised fraction ($\alpha(t)$), defined as the fraction crystallised at any time (t) follows the expression

$$a(t) = 1 - exp\left[-(Kt)^n\right] \tag{1}$$

Where n is the Avrami exponent which defines the mechanism and dimensionality of the crystal growth. K is the reaction rate constant and has an Arrhenius temperature dependency which has the form [18]

$$K = K_o \exp\left(\frac{-E_c}{RT}\right) \tag{2}$$

Where K_o, the pre-exponential factor usually referred to as the frequency factor indicates the frequency of attempts made by the nuclei to overcome the energy barrier during crystallisation, R is the universal gas constant and E_c is the activation energy for crystallisation. Several workers have advanced diverse models to calculate E_c based on the JMA model. One of the approaches is the observed linear dependence of $\ln(\beta/T_c^2)$ on $1/T_c$ observed by Kissinger [19] which has the form

$$\ln\frac{\beta}{T_c^2} = \text{constant} - \left(\frac{E_c}{RT_c}\right) \tag{3}$$

Where β is the constant heating rate. Matusita and Sakka [20] derived a non-isothermal method which linked the crystallised fraction (α) at any temperature T through the expression

$$\ln(1-a)^{-1} = \left(\frac{A}{\beta n}\right)\left[\frac{-nE_c}{RT}\right] \tag{4}$$

Where A is a constant. For a constant temperature, this equation can be written as [21]

$$\ln\left[-\ln(1-a)\right] = -n\ln\beta - 1.052mE_cRT + \text{constant}, \tag{5}$$

Where m is a constant that shows the growth mechanism. From this equation, the value of the n can be obtained by plotting $\ln[-\ln(1-a)]$ against $\ln a$ at the same temperature. Moreover at peak temperatures $T=T_c$, the values of α are independent of β [21] and (Eq. (4)) reduces to

$$\ln\beta = -\left(\frac{E_c}{RT_c}\right) + \text{constant} \tag{6}$$

In addition E_c can be evaluated from the approximation methods advanced by Augis and Bennett [22] which follows the expression

$$\ln\frac{\beta}{T_c} \cong -\left(\frac{E_c}{RT_c}\right) + \ln k_o \tag{7}$$

From this approximations value of E_c can be obtained from the linear plots of $\ln(\beta/T_c^2)$, $\ln(\beta/T_c)$ and $\ln\beta$, as a function of $1000/T_c$. The last expression (Eq. (7)) gives a linear plot with a y-intercept corresponding to $\ln K_o$ from which the pre-exponential factor K_o of the Arrhenius relation (Eq. (2)) can be obtained.

3.1. Moynihan's method

The dependence of T_g on β is interpreted in terms of thermal adjustments during glass transition and activation energy for glass transition. According to Moynihan's relation (Eq. (8)) [23], the enthalpy $H(T,t)$ is a function of temperature and time such that after an instantaneous isobaric change in temperature the system moves towards a new equilibrium $H_c(T)$ through isothermal relaxation which follows the relation

$$\left(\frac{dH}{dt}\right)_T = -\frac{(H-H_c)}{\tau} \tag{8}$$

Where τ is a parameter that is temperature dependent and is related to structural relaxation time through the expression

$$\tau = \tau_o exp\left(-\frac{E_t}{RT}\right) exp[-C(H-H_c)] \tag{9}$$

Where both τ_o and C are constants. From Eqs. (8) and (9), it has been shown that [24,25]

$$\frac{d\ln\beta}{d\left(\frac{1}{T_g}\right)} = -\frac{E_t}{R} \tag{10}$$

E_t can be obtained by plotting $\ln\beta$ against $1000/T_g$.

4. Results

Inset of Fig. 1 shows an XRD bitmap of $Se_{85}In_{15}$ confirming amorphous nature of the samples. Typical DSC thermographs of $Se_{100-x}In_x$ ($x=5, 10, 15, 20$) at heating rate of 15 K/min are shown in Fig. 1. Similar thermographs (not shown here) were obtained for other heating rates. The single glass transition and crystallisation peak indicate homogeneity of these glass samples.

Based on mean coordination number ($<Z>$) concept introduced by Philips [26], Thorpe [27] advanced a rigidity theory where he looked at a glass as consisting of a network of floppy and rigid regions. It was postulated that a transition will occur when the mean coordination number increases with rigidity percolation occurring throughout the network when $<Z>$ passes a value of 2.4. At this value the glass

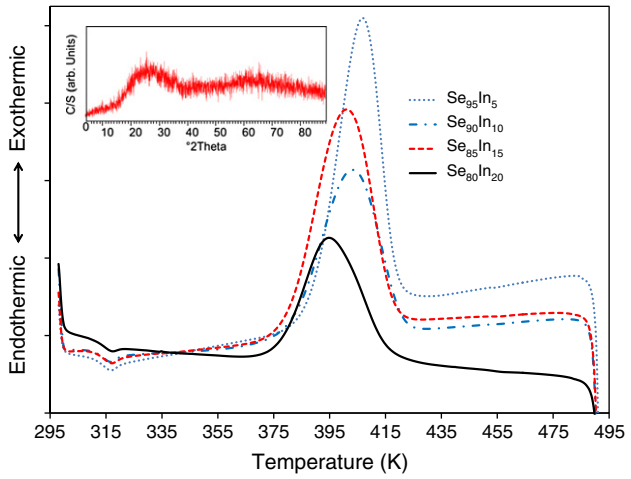

Fig. 1. DSC thermographs of $Se_{95}In_5$, $Se_{90}In_{10}$, $Se_{85}In_{15}$ and $Se_{80}In_{20}$ glassy alloys for a heating rate of 15 K/min. Inset: sample XRD bitmap of $Se_{85}In_{15}$. Lines drawn as guide to the eyes.

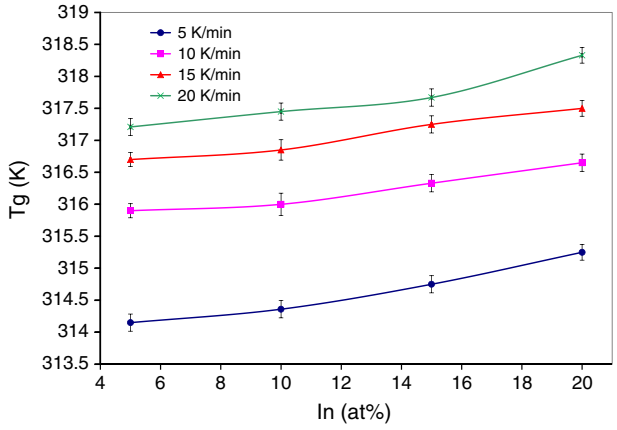

Fig. 2. Variation of T_g with indium content for $Se_{100-x}In_x$ for various heating rates. Lines drawn as guide to the eyes.

network changes from floppy glass to rigid glass. For a binary glass of the form $A_\alpha B_\beta$ as for the case of Se–In, <Z> can be evaluated from [27];

$$<Z>N = \frac{aN_A + \beta N_B}{a+\beta} \tag{11}$$

Where N_A and N_B are coordination numbers of elements A and B respectively. Values of <Z> are listed in Table 1. Indium has a coordination number of 5 as compared to that of Se which is 2. As theoretically anticipated, the calculated mean coordination numbers (Table 1) increase with In additive.

Fig. 2 shows T_g plotted as a function of indium content for $Se_{100-x}In_x$ for various heating rates. The plot reveals that T_g increases with addition of indium in the glassy alloys and heating rates. The values of T_g are well above room temperature and this is essential for applications based on phase changes as the alloys are anticipated to resist spontaneous transition around room temperature. T_g is a measure of rigidity of the network and is expected to rise with increased mean coordination number due to cross linking in the amorphous matrix, higher bond energies and variation of viscosity by changing composition in these glassy alloys [28,29]. For all the heating rates the crystallisation temperature T_c was found to decrease with increased In as revealed in Fig. 3.

T_g varies with the heating rates (β) and the relationship follows the empirical relationship suggested by Lasocka [30] which has the form

$$T_g = A + B\ln\beta \tag{12}$$

Where A is a constant that depicts the transition temperature at heating rate of 1 K/min and B is a constant that depends on the cooling rates during quenching. The significance of B is associated with response of changes in configurations in the vicinity of the glass forming region and usually decreases with decreasing cooling rates of the melts [31,32]. Fig. 4 shows a plot of T_g and $\ln\beta$ showing a linear relationship from which A and B can be determined. The same cooling rate was used for all the samples and hence the observed near invariance of B for all the samples. The values of A and B are summarised in Table 1.

It is well documented that E_t is responsible for configurational rearrangements of molecules/atoms around T_g and that glasses with lower E_t are more stable [33,34]. E_t can be obtained from Moynihan's relationship (Eq. (10)) from the slopes of linear plots of $\ln\beta$ and $1000/T_g$. Moynihan's plots are as shown in Fig. 5 for various $Se_{100-x}In_x$ alloys. Some workers [7] have successfully applied Kissinger's equation (Eq. (3)) in the form of Eq. (13) to obtain E_t.

$$ln\left(\frac{\beta}{T_g^2}\right) = \text{constant} - \left(\frac{E_t}{RT_g}\right) \tag{13}$$

Since this method is proposed for amorphous to crystalline transformation, the validity of application of this model in glass transition is not clear noting that glass transition is not a phase transformation but just a structural relaxation. Successful application of the Kissinger method with results close to Moynihan's method is quite interesting. In this work we have extended Augis–Bennett model (Eq. (7)) in the form of Eq. (14) to evaluate E_t.

$$ln\left(\frac{\beta}{T_g}\right) \cong \left(\frac{-E_t}{RT_g}\right) \tag{14}$$

Plots of $\ln\beta$, $\ln(\beta/T_g)$ and $\ln(\beta/T_g^2)$ as a function of $1000/T_g$ (Figs. 5–7) show a linear relationship. For the purpose of obtaining the slopes (Figs. 4–11), lines of best fit to the plotted points were drawn using Microsoft Excel 2010 and values confirmed with Originpro8 software. The values of E_t are listed in Table 1 and it is worth noting that the results obtained by the three methods are in close agreement which

Table 1
Activation energy for glass transition (E_t), Lasocka constants (A and B) and mean co-ordination number (<Z>) in glassy $Se_{100-x}In_x$.

	Activation energy for glass transition (E_t) kj mol^{-1}				Lasocka constants		
Alloy	Moynihan	Augis–Bennett	Kissinger	Mean	A (K)	B (min)	<Z>
$Se_{95}In_5$	368.63 ± 0.83	366.40 ± 4.08	368.08 ± 6.15	367.70 ± 3.68	310.6 ± 0.3	2.24 ± 0.2	2.15
$Se_{90}In_{10}$	371.13 ± 2.68	368.63 ± 7.09	365. 99 ± 4.89	368.58 ± 4.89	310.8 ± 0.3	2.23 ± 0.2	2.30
$Se_{85}In_{15}$	385.15 ± 1.52	382.53 ± 8.02	379.89 ± 9.20	382.52 ± 6.25	311.3 ± 0.3	2.14 ± 0.2	2.45
$Se_{80}In_{20}$	373.34 ± 2.66	370.81 ± 9.49	368.08 ± 9.79	370.74 ± 7.31	311.6 ± 0.3	2.23 ± 0.2	2.60

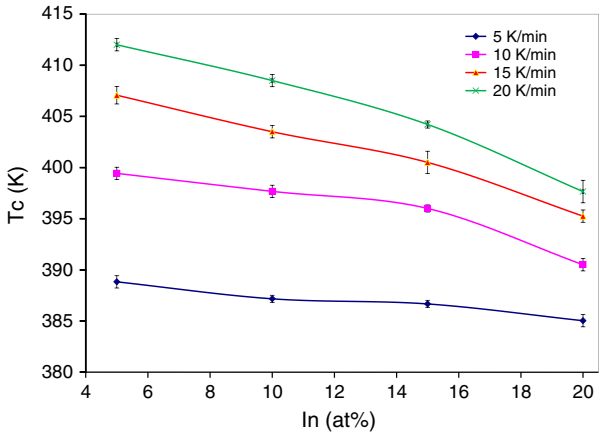

Fig. 3. Variation of T_c with In for $Se_{95}In_5$, $Se_{90}In_{10}$, $Se_{85}In_{15}$ and $Se_{80}In_{20}$ glassy alloys. Lines drawn as guide to the eyes.

implies the validity of these models in evaluation of activation energy for glass transition. However no proportionate dependence of E_t on In content was observed although there was a general increase of E_t between 5 and 15 at.%. Such near invariance of E_t on composition was observed by Tiwari et al. [33] for $Se_{1-x}Sb_x$ alloys. As earlier mentioned, increase in T_g is attributed to relative increase in mean coordination numbers, bond energies and molecular weight in these In richer chalcogenides.

The activation energy for crystallisation is a measure of potential for crystallisation and a recipe for consideration during applications.

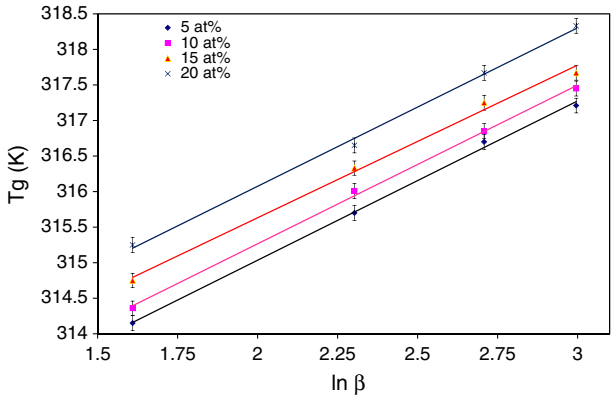

Fig. 4. Lasocka plots showing a linear relationship between T_g and lnβ.

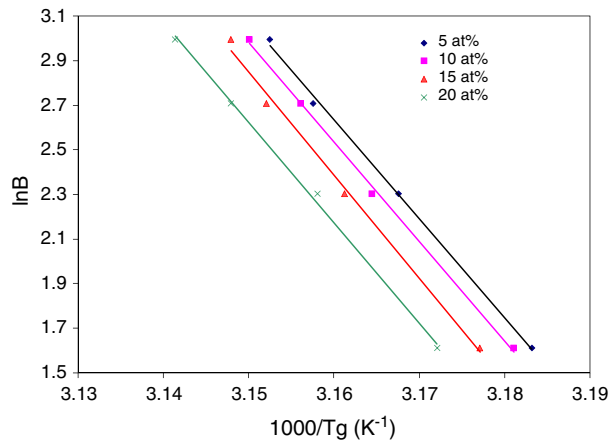

Fig. 5. Plot of lnβ versus $1000/T_g$ for $Se_{95}In_5$, $Se_{90}In_{10}$, $Se_{85}In_{15}$ and $Se_{80}In_{20}$ glassy alloys.

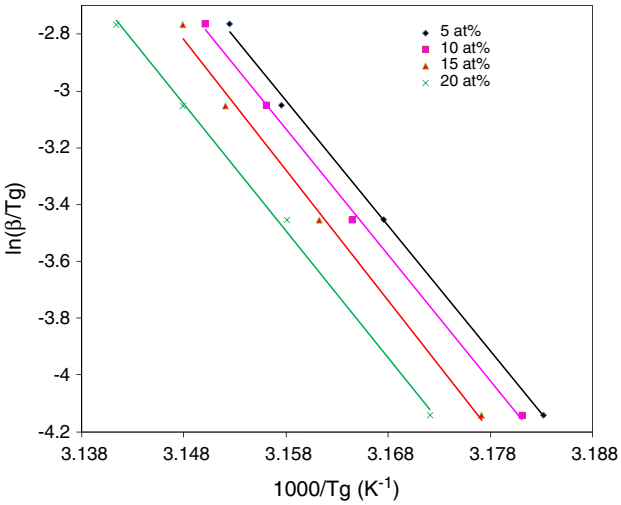

Fig. 6. Plot of $ln(\beta/T_g)$ versus $1000/T_g$ for $Se_{95}In_5$, $Se_{90}In_{10}$, $Se_{85}In_{15}$ and $Se_{80}In_{20}$ glassy alloys.

The activation energy for crystallisation was obtained using the Kissinger's, Augis–Bennett's and Mahedevan's methods by plotting $\ln(\beta/T_c^2)$, $\ln(\beta/T_c)$ and $\ln\beta$, as a function of $1000/T_c$ in Figs. 8, 9 and 10 respectively. The values of E_c were obtained from slopes of these linear plots and have been listed in Table 2. The obtained values show closeness of the results obtained which confirms the validity of these models as tools for evaluating E_c.

There was a notable a discontinuity of E_t and E_c at In = 15 at%. This discontinuity has been reported by others for various glass alloys and has been attributed to structural and chemical stabilities at certain mean coordination numbers [7,34]. The obtained values of E_t are higher than those of E_c which is consistent with results usually obtained [12,32,35,36] for these binary and ternary Se based chalcogenides. The frequency factor K_o was determined from the Arrhenius equation with knowledge of E_c and and $\ln K_o$ from the Augis–Bennett equation (Eq. (7)). These values are recorded in Table 2 and the reported range is in agreement with literature (Mehta et al. (Se–In, Se–Ge and Se–Te) [9], El-Oyoun (Ga–Se) [10] and Abdel-Rahim et al. (Bi–Se) [35]). K_o is a measure of probability of molecular collisions during crystallisation.

At constant temperature, $\ln[-\ln(1-\alpha)]$ versus $\ln\beta$ at different temperatures was plotted and from the slope of the relation the values of the order of the crystallisation mechanism or Avrami index (n) were

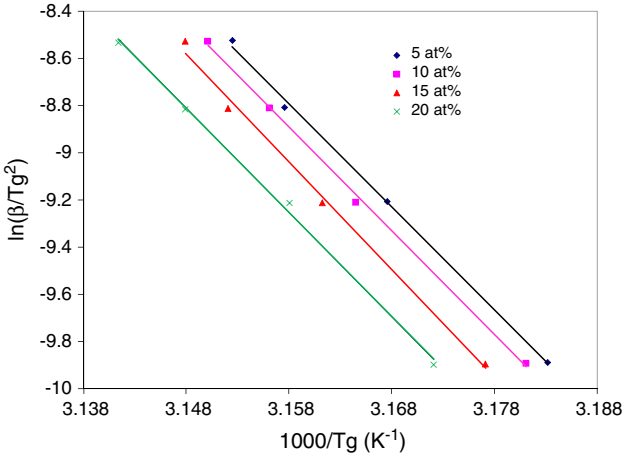

Fig. 7. Plot of $\ln(\beta/T_g^2)$ versus $1000/T_g$ for $Se_{95}In_5$, $Se_{90}In_{10}$, $Se_{85}In_{15}$ and $Se_{80}In_{20}$ glassy alloys.

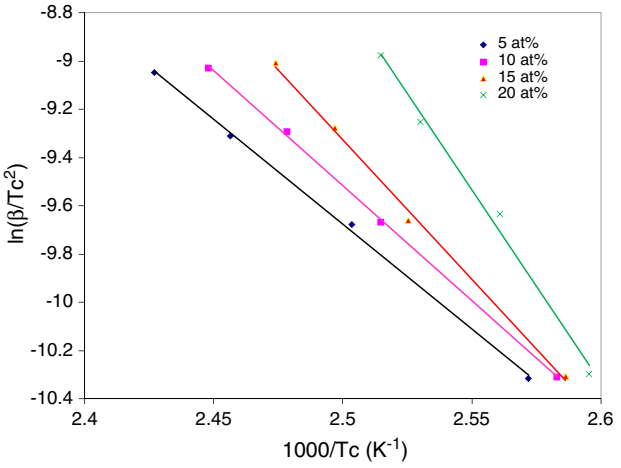

Fig. 8. Variation of $\ln(\beta/T_c^2)$ with $1000/T_c$ for $Se_{95}In_5$, $Se_{90}In_{10}$, $Se_{85}In_{15}$ and $Se_{80}In_{20}$ glassy alloys.

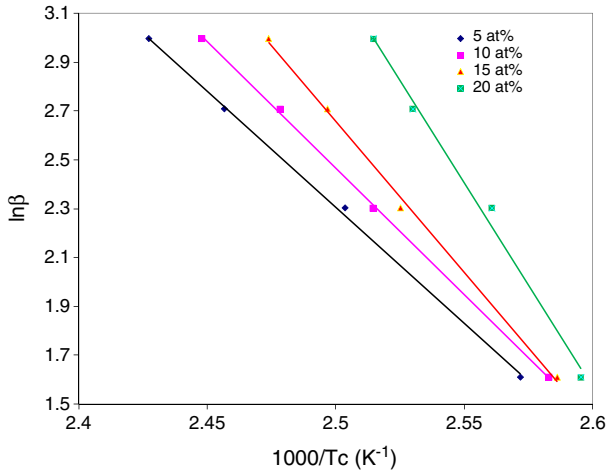

Fig. 10. Variation of $\ln\beta$ with $1000/T_c$ for $Se_{95}In_5$, $Se_{90}In_{10}$, $Se_{85}In_{15}$ and $Se_{80}In_{20}$ glassy alloys.

evaluated. The observed values obtained for $Se_{95}In_{15}$ were plotted in Fig. 11 and the full results listed as an inset table in Fig. 11. For samples where nucleation is not initiated prior to thermal analysis, the dimension of growth (m) is related to n through, $n=m+1$. The parameter $n=m$ for samples with nuclei prior to heating [10,31]. The observed values reveal that the dimension of growth is 2 dimensional ($n=3$) for $Se_{95}In_5$, 1($n=2$) for $Se_{90}In_{10}$ and 1($n=1$) for $Se_{85}In_{15}$ and $Se_{80}In_{20}$. Furthermore the values of n reduced with temperature and increased indium content which shows shift towards one dimensional growth with temperature which is brought about by nucleation saturation at higher temperatures. Increased In in the matrix shifts the crystallisation mechanism towards unity and predominantly towards growth driven crystallisation.

Glass forming ability (GFA) is the relative ability of the glass composition to conform to and remain in the amorphous state. Models derived for evaluating GFA and thermal stability of glasses are abundant in literature [37]. One of the major glass forming ability (GFA) indicators in amorphous materials is the temperature separation between T_g and T_c, $\Delta T_{cg}=(T_c-T_g)$ [38]. The observed values of ΔT_{cg} (Fig. 12) reduced with increased In for all the heating rates. The same trend was observed by Abdel et al. [35] for increased Bi in Se–Bi glassy system. Crystallisation starts after the glass has attained the characteristic onset of crystallisation temperature (T_o). At a faster crystallisation rate, the time required for the amorphous to complete crystalline transformation is smaller and therefore for a constant heating rate the peak crystallisation temperature is smaller. The observed relationship between crystallisation rate parameters $\ln K$ and ΔT_{cg} is opposite and therefore lower values of ΔT_{cg} are a measure of potential for the glass to pass into the crystalline state. Another GFA indicator is the glass forming factor K_{gl} also referred to as Hubry's number (H_r) [39] which for a glassy material is given by

$$K_{gl}=\left(\frac{T_c-T_g}{T_m-T_c}\right) \tag{15}$$

Where T_m is the peak melting temperature. Values of K_{gl} are plotted in Fig. 13 as a function of In concentration. It is not easy to prepare glasses for $K_{gl}\leq 0.1$. Good GFA is found for glasses with $K_{gl}\geq 0.4$ [39]. Higher values of T_c–T_g delays nucleation while smaller values of T_m–T_c retard growth after nucleation. Larger K_{gl} values are revealed at higher heating rates. The values of K_{gl} for a heating rate of 10 K/min were found to reduce from 0.57 at 5 at.% to 0.34 at 20 at.% In content. Therefore the GFA decreases with In content and falls sharply after In content greater than 15 at.% when mean co-ordination number (<Z>) increases above 2.4 (Table 1). The GFA was also evaluated by the reduced glass transition temperature, $T_{rg}=T_g/T_m=0.64$ [40,41].

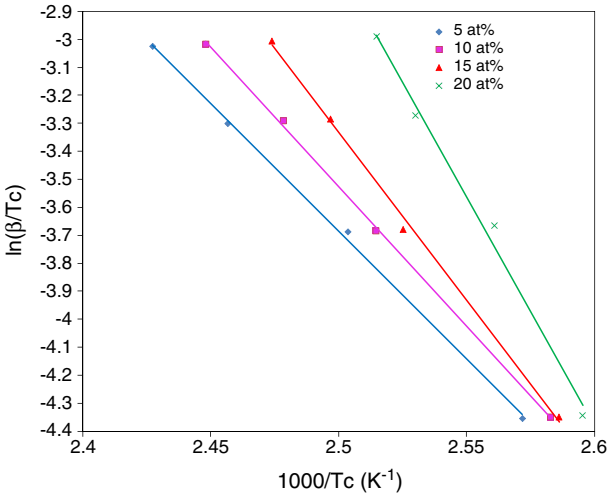

Fig. 9. Variation of $\ln(\beta/T_c)$ with $1000/T_c$ for $Se_{95}In_5$, $Se_{90}In_{10}$, $Se_{85}In_{15}$ and $Se_{80}In_{20}$ glassy.

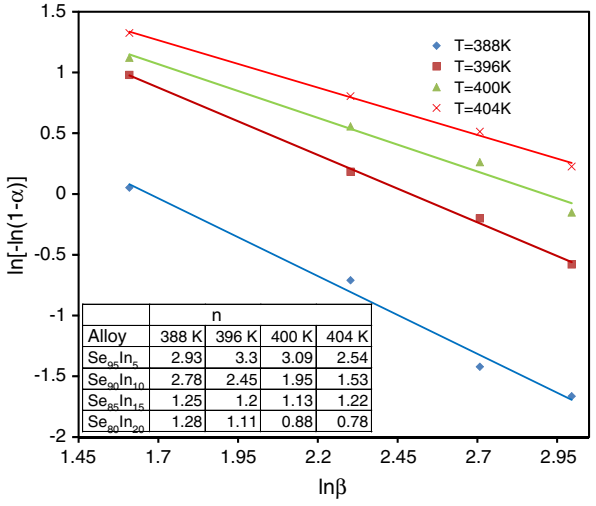

	n			
Alloy	388 K	396 K	400 K	404 K
$Se_{95}In_5$	2.93	3.3	3.09	2.54
$Se_{90}In_{10}$	2.78	2.45	1.95	1.53
$Se_{85}In_{15}$	1.25	1.2	1.13	1.22
$Se_{80}In_{20}$	1.28	1.11	0.88	0.78

Fig. 11. Plot of $\ln[-\ln(1-\alpha)]$ versus $\ln\beta$ for $Se_{95}In_5$, $Se_{90}In_{10}$, $Se_{85}In_{15}$ and $Se_{80}In_{20}$ glassy alloys. Inset: table of n values at different temperatures.

Table 2
Values of activation energy for crystallisation (E_c), frequency factor (K_o), and log of frequency factor ($\ln K_o$) for glassy $Se_{100-x}In_x$.

	Activation energy for glass crystallisation (E_c) kj mol^{-1}					
Alloy	Mahedevan	Augis–Bennett	Kissinger	Mean	ln K_o	K_o
$Se_{95}In_5$	79.19 ± 0.21	75.86 ± 0.63	75.53 ± 1.04	76.86 ± 0.63	19.12	2.18E + 08
$Se_{90}In_{10}$	86.07 ± 4.19	82.76 ± 4.51	79.46 ± 1.86	82.76 ± 3.52	21.36	1.89E + 09
$Se_{85}In_{15}$	102.90 ± 3.13	99.62 ± 3.18	96.33 ± 3.44	99.62 ± 3.25	26.62	3.64E + 11
$Se_{80}In_{20}$	139.60 ± 6.58	136.36 ± 3.34	133.11 ± 4.52	136.36 ± 4.81	38.26	4.13E + 16

This method, derived for organic polymers, also holds well for other systems such as inorganic glasses, oxides and sulphides [42]. The obtained values of T_{rg} (Table 3) follow the "two thirds rule" and reveal good adherence to this rule indicating good GFA.

The quantities that describe glass thermal stability are related to T_g, T_o and T_c and from these parameters, various quantitative methods have been advanced to bring insight into the degree of thermal stability in glassy alloys. One of the earliest thermal stability studies in glasses was by Dietzel [42] who used $\Delta T_{cg} = T_c - T_g$ and Saka and Mackezie [43] using T_g/T_m. Other later criterion included work done by Saad and Poulain [44] who postulated that the weighted glass thermal stability, H_w, and thermal stability parameter, S, are related with these stability indicators through

$$H_w = \frac{\Delta T_{cg}}{T_g} \tag{16}$$

$$S = \frac{(T_c - T_o)\Delta T_{cg}}{T_g} \tag{17}$$

Thermal parameter S reflects the resistance to devitrification after formation of the glass. The numerator has two terms (T_c–T_o) which are related to the rate of devitrification transformation of the glassy phase while the other term ΔT_{cg} retards the nucleation process. The values of S and T_g/T_m at different heating rates are given in Table 3 while plots of H_w with In content are shown in Fig. 14.

The fragility index (F_i) [45] is a measure of the rate at which relaxation time decreases with increasing temperature around T_g and is given by

$$F_i = \frac{E_t}{RT_g \ln(\beta)} \tag{18}$$

Strong glass forming liquids exhibit an approximate Arrhenius temperature dependence of the viscosity and have lower fragility values with a limit of $F_i \approx 16$ while the upper limit indicating kinetically fragile glass forming liquid, $F_i \approx 200$ [45]. The values of F_i for a heating rate of 10 K/min are presented in Fig. 15 and are in the range of 86.6–90.0 indicating that the studied compositions fall within moderately strong glass forming liquids. Strong glasses are those that show resistance to structural degradation in the liquid state at temperatures below T_g.

5. Discussion

The observed single glass transition and melting minima accompanied by a single crystallisation peak is typical of a homogeneous phase in the alloys. Glass transition is an endothermic reaction characterised by the absorption of heat and an increase in the atomic mobility with increasing temperature. At critical temperature, they get arranged in ordered patterns. When the polymer falls in these ordered patterns they release heat and an exothermic peak is observed with a maximum at the T_c. At T_m, the polymer crystals fall apart from the ordered patterns into free mobile states; latent heat of fusion is absorbed to break these ordered patterns. Unlike T_m, T_g depends on the speed of liquefaction and as such T_g is not uniquely defined so that glass transition is not a phase transition but rather an anomalous relaxation of disordered structures [7].

On a bonding perspective, intrinsic a-Se traditionally consists of two known structural configurations, helical chains of trigonal Se and rings of Se_8 consisting of monoclinic Se [2,28]. Factoring steric hindrances arising from difference in sizes of alloying atoms, larger atoms such as Bi, Sb and In initially (up to 1 at%) attach at the end of the chain increasing chain length and increasing T_g. Above the 1% limit, the extra atoms enter into the chain partially breaking down the long chains and hence increasing the proportion of Se_8 rings with consequent decrease in T_g [28]. The observed monotonic increase of T_g with addition of In above this limit was attributed to the crosslinking and the substitution of Se–Se homopolar bonds with Se–In heteropolar bonds with increased bond energies [36]

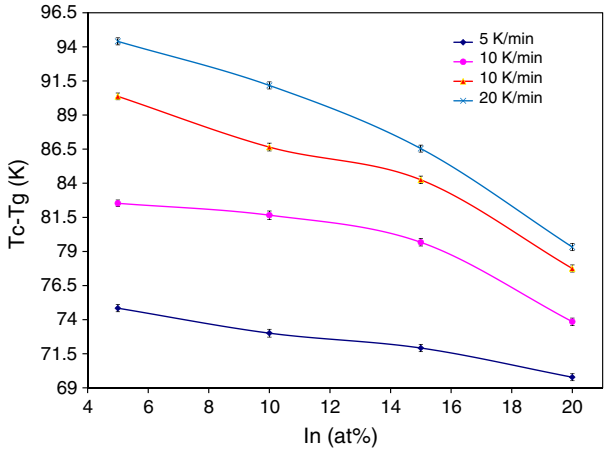

Fig. 12. Plot of ΔT_{cg} versus In content for different heating rates for $Se_{95}In_5$, $Se_{90}In_{10}$, $Se_{85}In_{15}$ and $Se_{80}In_{20}$ glassy alloys. Lines drawn as guide to the eyes.

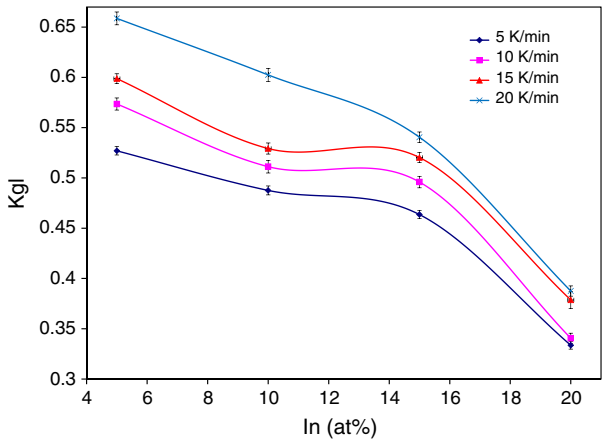

Fig. 13. Plot of glass forming factor (K_{gl}) versus In content for different heating rates for $Se_{95}In_5$, $Se_{90}In_{10}$, $Se_{85}In_{15}$ and $Se_{80}In_{20}$ glassy alloys. Lines drawn as guide to the eyes.

Table 3
Thermal stability parameters, reduced glass transition temperature (T_g/T_m), and crystallisation parameter (S) at various heating rates for $Se_{100-x}In_x$.

	5 K/min		10 K/Min		15 K/Min		20 K/Min	
Alloy	T_g/T_m	S (K)	T_g/T_m	S (K)	T_g/T_m	S (K)	T_g/T_m	S (K)
$Se_{95}In_5$	0.635 ± 0.0004	3.01 ± 0.07	0.639 ± 0.0004	4.59 ± 0.08	0.642 ± 0.0004	6.87 ± 0.10	0.642 ± 0.0004	7.13 ± 0.10
$Se_{90}In_{10}$	0.635 ± 0.0004	3.25 ± 0.08	0.639 ± 0.0005	5.51 ± 0.09	0.641 ± 0.0006	6.88 ± 0.10	0.641 ± 0.0005	7.04 ± 0.10
$Se_{85}In_{15}$	0.635 ± 0.0004	3.37 ± 0.07	0.639 ± 0.0005	5.12 ± 0.09	0.640 ± 0.0005	6.17 ± 0.09	0.641 ± 0.0004	6.60 ± 0.09
$Se_{80}In_{20}$	0.635 ± 0.0004	5.49 ± 0.08	0.639 ± 0.001	6.65 ± 0.10	0.641 ± 0.0005	7.10 ± 0.10	0.643 ± 0.0004	7.47 ± 0.09

from 43.81 kj mol^{-1} to 48.2 kj mol^{-1} respectively. It is established that in the quest to satisfy its co-ordination requirements, dissolution of In into the Se chains forms a cross linked matrix which increases the lattice rigidity, increasing T_g, and decreases thermal stability as well as T_c [31]. The increased values of T_g may also be a result of changes in the dihedral angles of the Se matrix due to crosslinking brought about by presence of In which increases configurational states to be overcome with consequent upward shift of T_g values [46].

As mentioned earlier the dimension of growth around the crystallisation peak shifted towards unity with increased temperature and indium content. Crystallisation of chalcogenide glasses is driven by nucleation and growth and α increases with increased temperature towards its maximum value of 1. It is worth mentioning

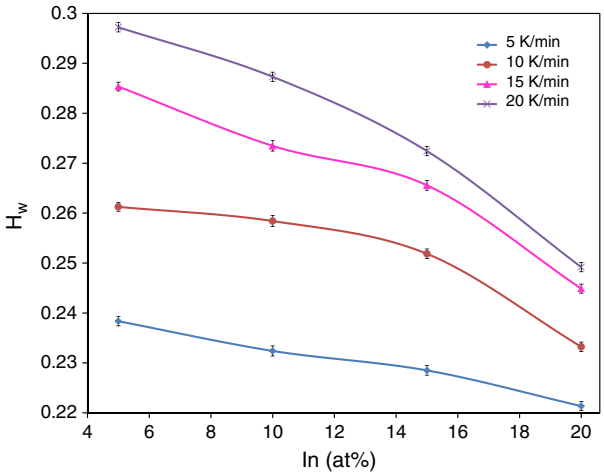

Fig. 14. Weighted thermal stability parameter (H_w) for different heating rates as a function of indium content. Lines drawn as guide to the eyes.

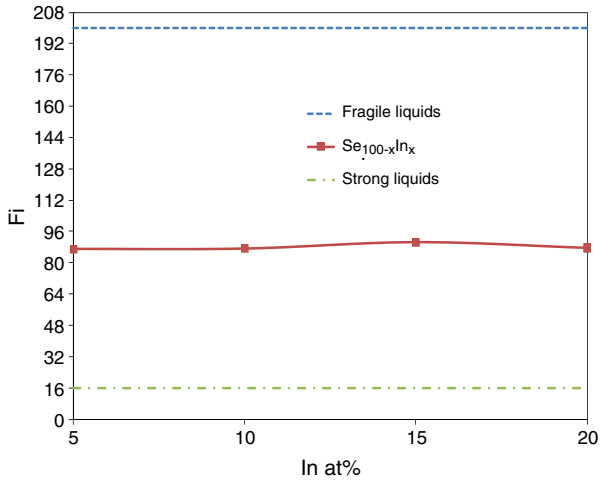

Fig. 15. Fragility index (Fi) parameter as a function of increasing indium content. Lines drawn as guide to the eyes.

that nucleation rate during crystallisation in DSC attains a maximum at temperatures higher than T_g and decreases with increasing temperature due to nucleation saturation. The rate of crystal growth attains maxima at a temperature much higher than the peak nucleation rate. Therefore, at constant heating, nuclei only form at lower temperatures and grow in size without further nucleation [2,10] hence a shift from nucleation driven around the onset of crystallisation to growth driven towards end of crystallisation. Therefore the obtained E_c values can be regarded as the effective activation energy for crystallisation encompassing a nucleation and growth component [2].

Thermal stability parameters include ΔT_{cg}, S, H_w and T_{rg} and their significance lies in the premises that the range of glass transition and accompanying temperature changes are important parameters to describe glass thermal stability. Higher values of these parameters imply higher thermal stabilities of these glasses. Of these, ΔT_{cg} is a strong indicator of thermal stability in that the higher the value, the more stable the glass [31,36,37]. In a study by Shabaan et al. [47] for $Ge_xIn_8Se_{92-x}$, it was concluded that glasses with highest stabilities were indicated by highest values of ΔT_{cg}, H_r and H_w and include those with $<Z> \leq 2.4$.

6. Conclusions

Non-isothermal calorimetry measurements have been performed in $Se_{100-x}In_x$ ($x = 5$, 10, 15, 20) glassy alloys. Various quantitative methods based on the JMA model have been used to evaluate E_t and E_c with close agreement implying the validity of these methods for determination of these parameters in the present system. The order parameter was dependent on composition and reduced towards unity with increased In content. A systematic increase of E_c was observed for increased indium concentration in the whole range studied. However no outright dependence of E_t was observed although there was a general increase of E_t between 5 and 15 at.%. The Augis–Bennett method was used to evaluate values of E_t and the obtained values are in agreement with the usual Moynihan's and Kissinger's methods. For the studied range, the GFA and thermal stability parameters calculated indicated less stable glasses for indium richer chalcogenide alloys.

Acknowledgements

The authors are grateful to the African Materials Science and Engineering Network (AMSEN)—a Carnegie IAS-Rise network and the University of Botswana for sponsoring this work.

References

[1] T. Wagner, S.O. Kasap, M. Vlcek, A. Sklen´ar, A. Stronski, J. Mat. Sci. 33 (1998) 5581.
[2] N. Mehta, M. Zulfequar, A. Kumar, Phys. Stat. Sol. 203 (2) (2005) 236 (a).
[3] E. Maruyama, Jpn. J. Appl. Phys. 21 (2) (1982) 213.
[4] J. Troles, V. Shiryaev, M. Churbanov, P. Houizot, L. Brilland, F. Desevedavy, F. Charpentier, T. Pain, G. Snopatin, J.L. Adam, Opt. Mater. 32 (2009) 212.
[5] B. Hyot, L. Poupinet, V. Gehanno, P.J. Desre, J. Magn. Magn. Mater. 249 (2002) 504.
[6] M. Saxena, J. Phys. D: Appl. Phys. 38 (2005) 460.
[7] S. Srivastava, M. Zulfequar, A. Kumar, Chalcogenide Lett 6 (8) (2009) 403.
[8] M.B. El-Den, Egypt. J. Sol. 24 (2) (2001) 171.
[9] N. Mehta, A. Kumar, J. Mater. Sci. 42 (2007) 490.

[10] M. Abu El-Oyoun, Phys B 406 (2011) 125.
[11] V.I. Mikla, V.V. Mikla, J. Mater. Sci. Mater. Electron. 20 (2009) 1095.
[12] N. Mehta, A. Kumar, J. Therm. Anal. Calorim. 87 (2) (2007) 343.
[13] G. Gordillo, C. Calderón, Sol. Energy Mater. Sol. Cells 77 (2) (2003) 163.
[14] H. Lee, Kang Dae-Hwan, L. Tran, Mater. Sci. Eng. B 119 (2005) 196.
[15] W.A. Johnson, R.F. Mehl, Trans. Am. Inst. Min. Metall. Eng. 135 (1939) 416.
[16] M. Avrami, J. Chem. Phys. 8 (1940) 212.
[17] M. Avrami, J. Chem. Phys. 7 (1939) 1103.
[18] M. Ahmad, R. Thangaraj, T.S. Sathiaraj, Eur. Phys. J. Appl. Phys. 47 (2009).
[19] H.E. Kissinger, Anal. Chem. 29 (11) (1957) 1702.
[20] K. Matusita, S. Sakka, Phys. Chem. Glasses 20 (1979) 81.
[21] S. Mahedevan, A. Giridhar, A.K. Singh, J. Non-Cryst. Solids 88 (1986) 11.
[22] A. Augis, J.E. Bennett, J. Therm. Anal. 13 (1978) 283.
[23] C.T. Moynihan, P.B. Macedo, C.J. Montrose, C.J. Montrose, P.K. Gupta, M.A. DeBolt, J.F. Dill, B.E. Dom, P.W. Drake, A.J. Easteal, P.B. Elterman, R.P. Moeller, H. Sasabe, J.A. Wilder, Ann. N. Y. Acad. Sci. 279 (1976) 15.
[24] S.O. Kasap, S. Yannacopoulos, J. Mater. Res. (1989) 893.
[25] S.O. Kasap, C. Juhasz, J. Mater. Sci. 21 (4) (1986) 1329.
[26] J.C. Phillips, J. Non-Cryst. Solids 34 (1979) 153.
[27] M.F. Thorpe, J. Non-Cryst. Solids 57 (1983) 355.
[28] D. Tonchev, S.O. Kasap, J. Non-Cryst. Solids 248 (1) (1999) 28.
[29] A. Omar, M. Lafi, M.A. Imran, M.K. Abdullah, Phys B 395 (2007) 69.
[30] M. Lasocka, Mater. Sci. Eng. 23 (2–3) (1976) 173.
[31] P.K. Jain, K.S. Deepika, N. Rathore, N.S. Jain, Saxena, Chalcogenide Lett 6 (3) (2009) 97.
[32] M.A. Abdel-Rahim, M.M. Hafiz, A.M. Shamekh, Phys B 369 (2005) 143.
[33] R.S. Tiwari, N. Mehta, R.K. Shukla, A. Kumar, Turk. J. Phys. 29 (2005) 233.
[34] H. Kumar, N. Mehta, A. Kumar, J. Term. Anal. Calorim 103 (2011) 903.
[35] M.A. Abdel-Rahim, A. El-Korashy, M.M. Hafiz, A.Z. Mahmoud, Phys B 403 (2008) 2956.
[36] M.M.A. Imran, N.S. Saxena, Y.K. Vijay, R. Vijay, R. Vijayvergiya, N.B. Maharjan, M. Husain, J. Non-Cryst. Solids 298 (2002) 53.
[37] N. Mehta, R.S. Tiwari, A. Kumar, Mater. Res. Bull. 41 (2006) 1664.
[38] S.A. Fayek, M. Fadel, J. Ovonic Res. 5 (2) (2009) 43.
[39] A. Hrubý, J. Czech. J. Phys. 22 (11) (1972) 1187.
[40] W. Kauzmann, Chem. Rev. 43 (2) (1948) 219.
[41] G. Kaur, T. Komatsu, R. Thangaraj, J. Mater. Sci. 35 (4) (2000) 903.
[42] A. Dietzel, Glass Tech. Ber. 22 (1968) 41.
[43] S. Sakka, J.D. Mackenzie, J. Non-Cryst. Solids 6 (1971) 145.
[44] M. Saad, M. Poulain, Mater. Sci. Forum 11 (1987) 19.
[45] M.M. Wakkad, E.K. Shokr, S.H. Mohamed, J. Non-Cryst. Solids 65 (1) (2000) 157.
[46] Y. Wang, P. Bochand, M. Micoulaut, Europhys. Lett. 52 (6) (2000) 633.
[47] E.R. Shaaban, I.S. Yahia, M. Fadel, J. Alloys Compd. 469 (2009) 427.